ChemCatChem

The European Society Journal for Catalysis

Chemistry Europe

European Chemical Societies Publishing

Supported by GECATS GERMAN CATALYSIS SOCIETY

Accepted Article

Title: COx-resistant oxidative dehydrogenation of Cyclohexane catalyzed by sp3@sp2 Nanodiamonds towards highly selective Cyclohexene production

Authors: Pengfei Du, Xin-Xing Zhang, Shaoqian Zhang, Yang Zhao, Liyun Zhang, Bingsen Zhang, and Bing Yang

To be cited as: *ChemCatChem* 10.1002/cctc.202001380

Link to VoR: https://doi.org/10.1002/cctc.202001380

WILEY-VCH

10.1002/cctc.202001380

WILEY-VCH

FULL PAPER

CO_x-resistant oxidative dehydrogenation of Cyclohexane catalyzed by $sp^3@sp^2$ Nanodiamonds towards highly selective Cyclohexene production

Pengfei Du[a],[b],# Xin-Xing Zhang[c],#, Shaoqian Zhang[d],Yang Zhao[a], Liyun Zhang[e], Bingsen Zhang[e], Bing Yang[a],*

Dedication: This work is dedicated to the memory of Prof. Dangsheng Su.

[a] Mr. P. F. Du,# Mr. Y. Zhao, Prof. Dr. B. Yang,*
Dalian National Laboratory for Clean Energy
Dalian Institute of Chemical Physics, Chinese Academy of Science
457 Zhongshan Road, Dalian 116023 (China)
* E-mail: byang@dicp.ac.cn
[b] Mr. P. F. Du
University of Chinese Academy of Sciences
19 Yuquan Road, Beijing 100049 (China)
[c] Dr. X.-X. Zhang, #
Department of Chemistry, James Franck Institute and Institute for Biophysical Dynamics, The University of Chicago
929 E 57th Street, Chicago, Illinois 60637 (United States)
[d] Dr. S. Q. Zhang
Key Laboratory of Chemical Lasers
Dalian Institute of Chemical Physics, Chinese Academy of Science
457 Zhongshan Road, Dalian 116023 (China)
[e] Dr. L. Y. Zhang, Prof. B. S. Zhang
Shenyang National Laboratory for Materials Science
Institute of Metal Research, Chinese Academy of Sciences
72 Wenhua Road, Shenyang (110016) China

# These authors contributed equally to this work

Supporting information for this article is given via a link at the end of the document.

Abstract: Deep oxidation/dehydrogenation are longstanding problems for decades in catalytic oxidative dehydrogenation (ODH) of cyclohexane and other alkanes. Here we show a metal-free catalyst of nanodiamonds (NDs) with unique $sp^3@sp^2$ hybrid structure that catalyzes CO_x-resistant cyclohexane ODH with remarkable reactivity towards cyclohexene production. The selectivity of cyclohexene can reach as high as 67% with significantly suppressed CO_x emission (< 5%), which is on top of the highest reported values among other metal(oxide)/metal-free catalysts. Structural evolution of $sp^3@sp^2$ NDs under annealing treatments and their specific surface functional groups are systematically studied using TEM, XPS, Raman and TPD. By comparing with carbon nanotubes (CNTs), we found that the carbonyl groups stabilized on strained $sp^3@sp^2$ core-shell NDs enhanced the cyclohexene selectivity via preferential cleavage of C-H over C-C bond. Kinetic studies further revealed the underlying reaction pathways that cyclohexane is rapidly dehydrogenated to cyclohexene which subsequently transforms into benzene (fast) and CO_x (slow). Deep oxidation of both cyclic hydrocarbons is largely suppressed due to the low density of electrophilic functional groups on strongly curved graphitic surface of $sp^3@sp^2$ NDs.

1. Introduction

Cyclohexene is one significant chemical in chemical engineering, textile and pharmaceutical industry,[1] and an important raw material for the production of cyclohexanol,[2] adipic acid,[2a] with a global demand of over 3 million tons per year.[3],[4] At present, cyclohexene is primarily produced via cyclohexanol dehydration using concentrated sulfuric acid in industry, which is low in efficiency and environmentally unfriendly.[5] Oxidative dehydrogenation (ODH) of cyclohexane is an alternative and more efficient route to produce cyclohexene, which yields benzene and CO_x as byproducts.[6] As the concept of green chemistry,[7] the as-produced benzene can be recycled and hydrogenated to cyclohexene and cyclohexane, forming a close loop for cyclic production of cyclohexene (see Figure 1). Herein, CO_x is a fatal byproduct that results in irreversible carbon loss and the emission of greenhouse gases. Hence, to prevent CO_x formation in cyclohexane ODH reaction is highly demanded as to enhance the recyclability of benzene and thus the yield of cyclohexene.

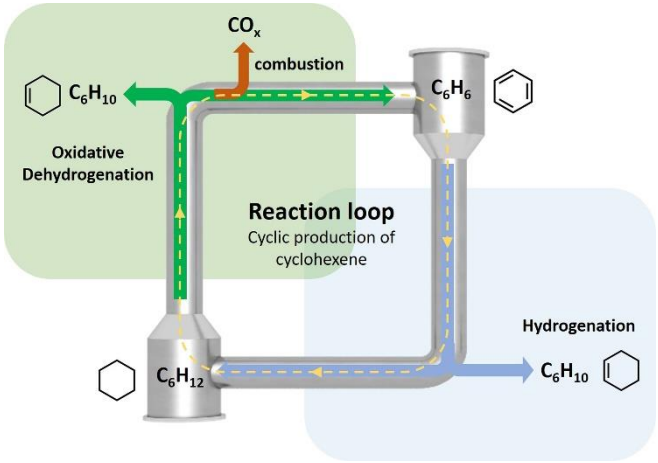

Figure 1. Reaction loop of Cyclohexane ODH incorporated with benzene hydrogenation towards green production of cyclohexene.

Metal/metal oxide catalysts are commonly used catalysts for ODH of cyclohexane.[1d, 6c, 6e, 8] However, deep oxidation and dehydrogenation [9] often occur inevitably yielding undesired CO_x and benzene as byproducts. On noble metal catalysts such as Au and Pd, strong C-H dissociation consequentially leads to deep dehydrogenation with overwhelming benzene selectivity (>86%) despite high conversion.[6d, 9c] Metal oxide catalysts e.g. vanadia however are prone to combustion yielding over 20% of CO_x due to their high affinity to C-C bond dissociation.[10] In recent years, metal-free carbon materials have attracted extensive interests because of their superior reactivity, diversity of active surface species [11] and sustainability.[12] Among those, nanodiamonds (NDs) are promising candidates due to their excellent chemical stability, higher surface area, and unique curvature,[13] showing remarkable catalytic performance in dehydrogenation of ethylbenzene,[14] butane,[15] propane,[16] and ethane[17]. However, ODH of cyclohexane has been rarely explored. Moreover, though earlier studies have presented the structure dependent reactivity of NDs in ODH reactions,[12, 18] the specific role of surface functional groups and the underlying mechanism for C-H and C-C dissociation remain to be elucidated.

Here we report a CO_x-resistant ODH of cyclohexane with remarkably high cyclohexene selectivity, catalyzed by metal-free NDs with tuned sp^3@sp^2 core–shell structure. The catalytic evaluation reveals that sp^3@sp^2 NDs has superior activity and the highest C_6/cyclohexene selectivity among other reported metal/metal oxide catalysts. Utilizing various characterization techniques including high resolution transmission electron microscope (TEM), X-ray photoelectron spectroscopy (XPS), X-ray diffraction (XRD) and temperature programmed desorption (TPD), the surface functional groups on sp^3@sp^2 NDs and their specific role in C-H and C-C dissociation during ODH reaction has been systematically investigated. Kinetic studies have been performed to further elucidate the reaction pathway and the underlying mechanism for CO_x resistance in ODH of cyclohexane.

Results and Discussion

2.1 Structural characterization of sp^3@sp^2 core–shell NDs.

The sp^3@sp^2 core–shell NDs were obtained by annealing in Ar atmosphere at elevated temperatures, i.e. 900 °C, 1100 °C, 1200 °C, and 1500 °C, denoted as NDs-900, NDs-1100, NDs-1200, and NDs-1500, respectively. (particle size: 3-10nm; pore volume:0.9-1.4 cm^3 g^{-1}) The structure evolution of NDs with increasing annealing temperature is displayed in Figure 2. The high-resolution transmission electron microscopy (HRTEM) image of the pristine NDs (untreated, Figure 2a) presents sp^3-structured ND particles covered by a thin layer of amorphous carbon, showing a characteristic spacing of 0.208 nm as (111) plane of sp^3-diamond. After annealing to 900 °C, the sp^3 feature remains despite the removal of the amorphous carbon layer (NDs-900, Figure S1a).

By further annealing, a growth of sp^2 graphitic shell is gradually observed on the outer surface of NDs-1100 and NDs-1200, as indicated by the emerging (002) plane of sp^2-graphite (Figure S1b and Figure 2b), forming sp^3@sp^2 core–shell nanostructure. Eventually at 1500 °C (Figure 2c), sp^2 structure becomes dominant, resulting in an onion-like carbon (OLC) structure on NDs-1500. The XRD patterns (Figure 2d) further confirm this structure evolution. The X-ray photoelectron spectroscopy (XPS) and Raman spectroscopy were further performed to reveal the surface structure and the corresponding surface functional groups. (see Figure 2d and the fitting results in supplementary discussion) The gradual increase of sp^2 carbon (%) deduced from XPS verifies the formation of the sp^2 shell. The evolution of oxygen containing surface groups reflects their thermal stability upon high temperature annealing, in an order of carboxyl < phenolic hydroxyl < carbonyl. The I_D/I_G ratio in Raman spectra (see Figure S3 and the supplementary discussion) was employed to reveal the degree of surface defects.[19] According to Table S1 and Figure 2e, NDs-1200 shows the highest degree of surface defects likely due to the lattice mismatch at the sp^3@sp^2 interface.[20] The formation of sp^2 dominated OLC structure on NDs-1500 results in less defects and a significant loss of surface OH and COOH groups. The ICP-MS analysis shows only a trace of impurities of alkali and transition metal (1~100 ppm level in wt%) with almost identical amount in all the NDs catalysts (see Table S2).

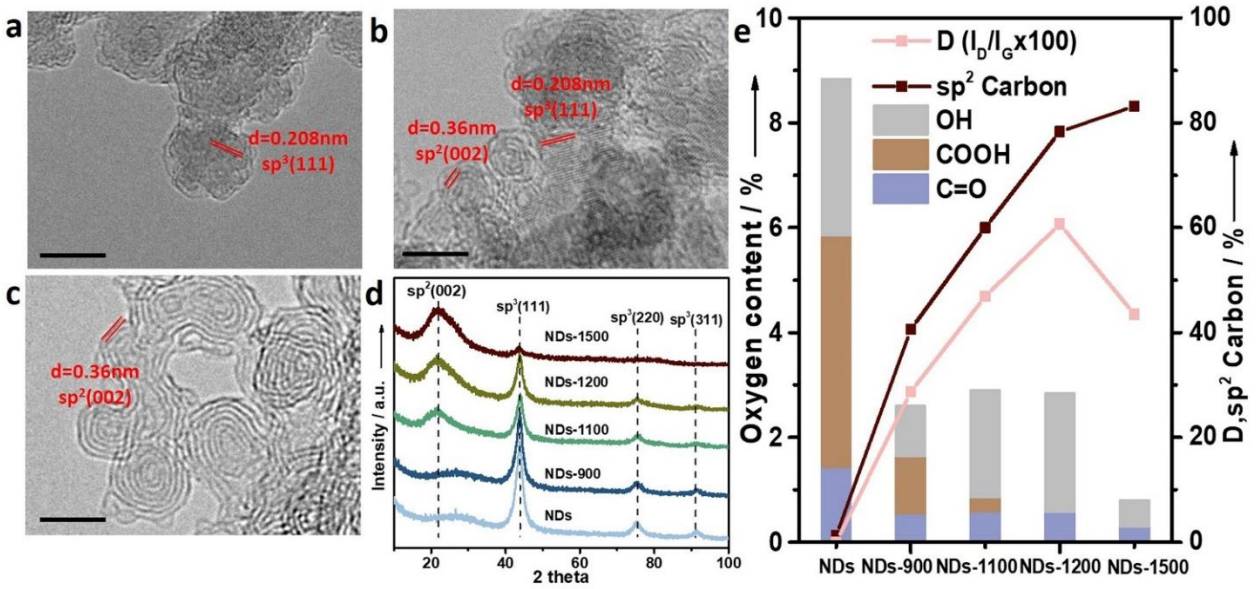

Figure 2. Structural characterization of NDs with various sp^3/sp^2 hybrid structure. HRTEM images (a-c); (a) NDs. (b) NDs-1200. (c) NDs-1500. Inserted scale bar: 5nm. (d) XRD patterns. (e) Evolution of surface structure and functional groups. The sp^2 carbon and relative oxygen content are deduced from XPS spectra. Defect degree is deduced from I_D/I_G signal in Raman spectra.

2.2 CO_x-resistant and highly selective ODH of cyclohexane.

Catalytic tests of all ND catalysts were carried out in a fix-bed reactor with a gas flow of 28 sccm of 1.4%C_6H_{12}/1.4%O_2/97.2%He. The measured activity and selectivity are summarized in Figure S5. Taking NDs-1200 for example (Figure 3a), the conversion of cyclohexane increases with temperature above 300 °C and reaches its maxima of 20.1% at 460 °C. In terms of selectivity, NDs-1200 exhibits excellent C_6 selectivity over 95% and highly suppressed CO_x production below 5%. (C_6 selectivity represents the sum of selectivity of benzene and cyclohexene) A slightly decreasing trend of C_6 selectivity is observed for all ND catalysts (Figure S5b) as the combustion reaction occurs to favor CO_x formation at elevated temperatures. The selectivity of C_6H_{10} on NDs-1200 remains above 60% up to 400 °C and then drops dramatically due to the preference of benzene formation at higher temperatures via deep dehydrogenation. In comparison, the conversion and selectivity at 460 °C of all ND catalysts are presented in Figure 3b. A volcano shape of cyclohexane conversion with respect to the annealing temperature of NDs is identified where NDs-1200 shows the highest activity, while NDs-1500 shows the highest C_6H_{10} selectivity of~ 67% among all tested ND catalysts. (see more detailed information in Figure S6 and S7) Both NDs-1200 and NDs-1500 exhibit the highest C_6 selectivity over 93% suggesting significantly suppressed CO_x formation on the annealed NDs.

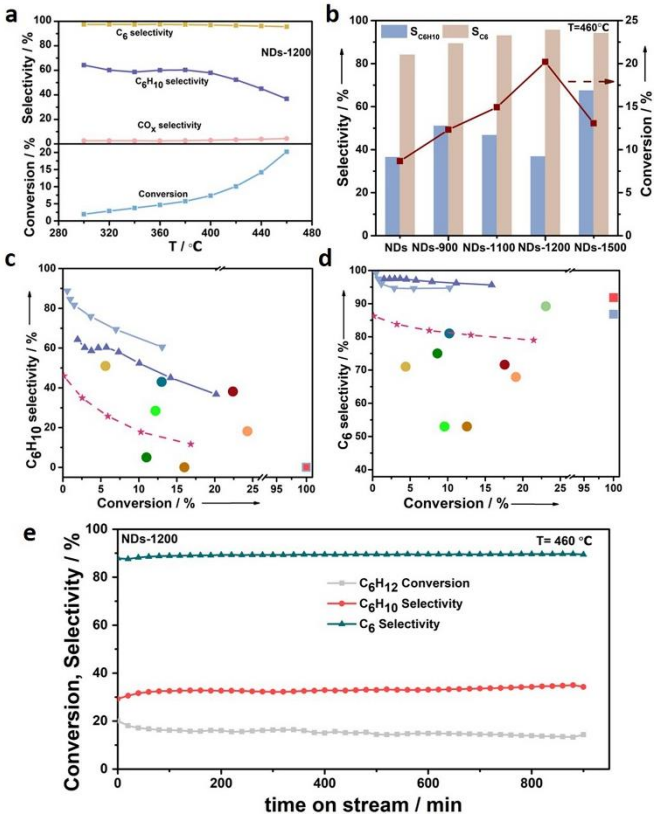

CNTs; NDs-1200; NDs-1500; CuO/KIT-6;[21] Fe_2O_3;[10b] $Mg_3(VO_4)_2$;[22] MnO_x/PC;[23] VO_x/Al_2O_3;[9a] Ce/AlO_x;[24] 5% FePc/γ-Al_2O_3;[10a] 5% Au/TiO_2;[6d] 5% Pd/TiO_2.[6d]

Figure 3. The catalytic performance of ND catalysts and the comparison with previous published works. (a) The conversion and selectivity of NDs-1200. (b) Comparison of reactivity between the ND catalysts, T=460 °C. C_6H_{10} selectivity (c) and C_6 selectivity (d) versus conversion plot of ND catalysts in this work, in comparison with other metal/metal oxide catalysts from previously published literatures. Squares and circles represent noble metal and metal oxide catalysts,

respectively. (e) The time-on-stream stability test of NDs-1200 under reaction condition at 460 °C.

Furthermore, the selectivity versus conversion plot is displayed in Figure 3 c and d for C_6 and cyclohexene, respectively. The ND catalysts i.e. NDs-1200 and NDs-1500 exhibit the topmost selectivity over a wide range of conversion among other metal/metal oxide catalysts from literatures and metal-free carbon nanotubes (CNTs) in this work (see thermal stability of NDs and CNTs in Figure S8), resulting in the highest yield of cyclohexene and over 93% C_6 selectivity. Supported metal catalysts such as Au and Pd,[6d] usually show over 95% conversion in cyclohexane ODH due to their excellent ability in C-H cleavage,[25] but the selectivity of cyclohexene is rather low (<5%) leading to primary benzene production (> 85%) via deep dehydrogenation.[6d] (see Table S3) In contrary, metal oxide catalysts e.g. ferric oxide,[10b] cerium oxide[10a, 24] and vanadium oxide[9a] exhibit much better cyclohexene selectivity (~50%) compared to noble metal, but the combustion on oxide catalysts is more pronounced as a result of over 20% CO_x (see Table S3). In addition, as metal-free catalyst, sp^3@sp^2 NDs also exhibit outstanding catalytic performance over the CNTs (see Table S3 and Figure S9), with outperformed selectivity of both C_6 and C_6H_{10}. Overall, we can conclude that the NDs suppress both deep oxidation and deep dehydrogenation of cyclohexane, leading to remarkable cyclohexene selectivity and inhibited CO_x production.

The long-term stability test was further performed on NDs-1200 catalyst at 460 °C with time on stream up to 15hr, as presented in Figure 3e. During the initial reaction period of ~2hr, the conversion of cyclohexane slightly drops likely due to the loss of some unstable surface groups such as carboxyls, which further results in less combustion and thus an increase of both C_6 and C_6H_{10} selectivity. Afterwards, NDs-1200 catalyst show an excellent C_6 and C_6H_{10} selectivity kept at ~92% and ~35%, with a stable conversion of ~15% for the rest of the test. To further demonstrate the structural stability of the ND catalysts, we have performed a full characterization of TEM, XRD, XPS and Raman spectroscopy for all the spent catalyst after reaction. (see Figure S10 and S11) A higher graphitization (sp^2) degree and oxygen content on the spent catalyst were clearly observed (Table S4), reflecting an enrichment of onion-like sp^2 carbon shell and oxygen functonal groups formed during reaction. This strongly indicates the significant role of curved sp^2 shell in promoting oxygen functonal groups for enhanced reactivtity in ODH of cyclohexane.

2.3 Structure-reactivity relationship of NDs.

The structure-reactivity relationship of all ND catalysts is displayed in Figure 4a. The conversion of cyclohexane and I_D/I_G signal show a similar volcano shape with a maximum on NDs-1200. This infers that the surface defect sites on the sp^3@sp^2 hybrid structures are likely responsible for the activity of cyclohexane ODH facilitated by the formation of oxygen functional groups during reaction.[17, 26] Moreover, the growing tendency of C_6 selectivity goes in line with the sp^2 content in NDs upon annealing, suggesting that the combustion reaction is largely suppressed on sp^2-graphite rather than sp^3-diamond structure.[17, 27]

In order to reveal the role of different surface functional groups in cyclohexane ODH, we have performed a control experiment by comparing the production rate of each product with CNTs at 460 °C. As a result, CNTs show much lower cyclohexene selectivity, and more pronounced CO_x production. (see Figure 4b) TPD spectra of spent NDs-1200, NDs-1500 and CNTs catalyst (Figure S12 and S13) enable the discrimination of different surface functional groups by referring to their characteristic desorption features. [18b, 28] As shown in Figure 4c and Table S5, both NDs-1200 and NDs-1500 spent catalysts favor the higher contents of carbonyl groups (-C=O) that promotes the dehydrogenation reaction via C-H bond dissociation, whereas the higher ratio of electrophilic groups (carboxyl and anhydride) on the spent CNTs catalyst in contrary facilitates the C=C bond breaking, consequently leading to an aggravated CO formation.[15, 18b, 26] The higher selectivity of cyclohexene over benzene on NDs-1200 and NDs-1500 indicates that the strained sp^3@sp^2 hybrid structure can effectively slow down the deep dehydrogenation of cyclohexene to yield benzene.

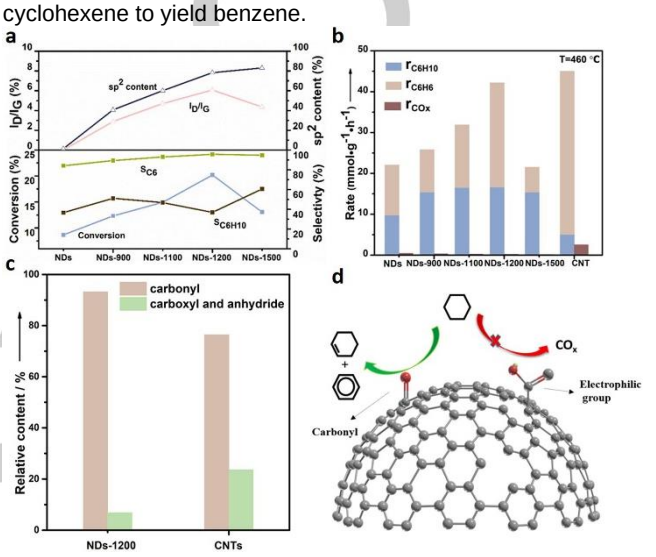

Figure 4. Structure-reactivity relationship of NDs in cyclohexane ODH. (a) Structure-reactivity relationship of NDs, T= 460 °C. (b) Production rate of C_6H_{10}, C_6H_6 and CO_x on NDs and CNTs, T= 460 °C. (c) Relative contents of surface functional groups on NDs-1200, NDs-1500 and CNTs after reaction. (d) Scheme of reaction path and active surface groups for cyclohexane ODH.

2.4 Kinetic Study.

To clarify the reaction pathways and the origin of high selectivity on the ND catalysts, we carried out a kinetic study on NDs-1500 by performing three independent oxidation reactions with cyclohexane, cyclohexene and benzene. Based on the catalytic testing results (Figure S14), the reaction rate for each product (T=460 °C) is displayed in Figure 5a. The kinetic analysis of each elementary reaction (Figure 5b) is described detailedly in the supplementary discussion by an simplified assumption of a first order reaction, as previously adopted elsewhere.[9a] The calculated rate constants for each elementary step i.e. k_1~ k_6 are summarized in Table S6. Here we notice that k_2, k_5, and k_6 are negligible, inferring that the reaction path of deep dehydrogenation directly from cyclohexane to benzene, and the combustion of cyclohexane and benzene are unfavorable on the ND catalyst. As plotted in Figure 5c, k_1, k_3, and k_4 increase with rising temperatures, and the magnitude is in an order of $k_3 > k_4 > k_1$ (>> k_2, k_5, k_6), revealing that cyclohexane is firstly dehydrogenated to cyclohexene (medium rate), which subsequently converts to benzene (fast rate) and CO_x (slow rate). It thus suggests that cyclohexene is a crucial intermediate which is responsible for byproduct formation. Furthermore, the activation barrier (E_a) for each reaction path is calculated using

the Arrhenius equation, as shown in Figure 5d. The similarity of Ea_1 (cyclohexane to cyclohexene) and Ea_3 (cyclohexene to benzene) i.e.164.2±8.9 kJ/mol and 178.8±1.3 kJ/mol reflects the same origin of active sites (carbonyl group) for dehydrogenation reaction. The lower Ea_4 (98.3±7.2 kJ/mol) for CO_x formation can be attributed to the exothermic nature of the combustion reaction, but the number of active sites (electrophilic functional groups) are significantly reduced as indicated by the small pre-exponential factor (Table S7).

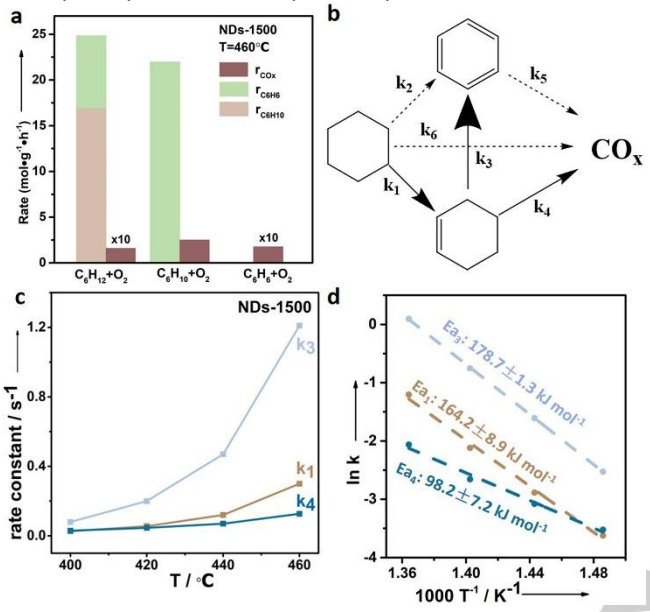

Figure 5. Kinetic study of cyclohexane (ODH) on the NDs-1500 catalyst. (a) Production rate of cyclohexene, benzene and CO_x at 460 °C in the oxidation reaction of cyclohexane, cyclohexene and benzene. (b) Schematic reaction pathways in cyclohexane ODH; solid lines represent the main pathways and the size of arrows indicates the magnitude of the rate constant. (c) The rate constants of k_1, k_3 and k_4 with increasing reaction temperature. (d) Arrhenius plot and the activation barriers calculated for different reaction pathways.

3. Conclusion

In this work, a systematic study of the ND catalysts with various sp^3/sp^2 nanostructures was carried out for the catalytic ODH of cyclohexane. The $sp^3@sp^2$ core–shell ND catalysts exhibit an outperformed catalytic reactivity among other reported catalysts in ODH of cyclohexane, with remarkably high cyclohexene selectivity (~67%) and suppressed CO_x formation (<5%). The structure-reactivity relationship further reveals the role of defect sites in stabilizing oxygen functional groups (nucleophilic species) during reaction that are highly active for ODH of cyclohexane. Compared with CNTs, we find that the curved structure of $sp^3@sp^2$ hybrid NDs can slow down deep dehydrogenation (C-H bond breaking), and further prevent the formation of carboxyl groups that leads to the combustion products (C=C bond breaking). Kinetic studies further reveal the reaction path, in which cyclohexane is firstly dehydrogenated to cyclohexene which is then converted to benzene (fast rate) and CO_x (slow rate).

Supporting information

Experimental details and characterization details; XPS, Raman, He TPD and the kinetic analysis were summarized in the supporting information.

Acknowledgements

This work received financial support from Talents Innovation Project of Dalian (2016RD04), Natural Science Foundation of China (21872145) and the Foundation of Dalian Institute of Chemical Physics (DICP I201943). This work is dedicated to the memory of Prof. Dangsheng Su for his valuable support and fruitful discussion.

Conflict of interest

The authors declare no competing financial interest.

Keywords: Cyclohexane, CO_x-resistant oxidative dehydrogenation, cyclohexene, $sp^3@sp^2$ nano-diamonds

[1] a) Y. Izawa, D. Pun, S. S. Stahl, *Science* **2011**, *333*, 209-213; b) U. Schuchardt, D. Cardoso, R. Sercheli, R. Pereira, R.S. da Cruzd, M. C. Guerreiro, E. V. Spinacé, E. L. Pires, *Appl. Catal. A* **2001**, *211*, 1-17; c) A. V. Losub, S. S. Stahl, *J. Am. Chem. Soc.* **2015**, *137*, 3454-3457; d) M. A. Andrade, L. M. D. R. S. Martins, *Catalysts* **2019**, *10*, 1-33.

[2] a) Y. Cao, H. Yu, J. Tan, F. Peng, H. Wang, J. Li, W. Zheng, N. B. Wong, *Carbon* **2013**, *57*, 433-442; b) H. M. AbdelDayem, M. Faiz, H. S. Abdel-Samad, S. A. Hassan, *J. Rare Earths* **2015**, *33*, 611-618.

[3] L. Wang, S. He, L. Wang, Y. Lei, X. Meng, F.S. Xiao, *ACS Catal.* **2019**, *9*, 11335-11340.

[4] J. Yang, J. Liu, H. Neumann, R. Franke, R. Jackstell, M. Beller, *Science* **2019**, *20*, 1514-1517.

[5] D. Wang, X. Shu, M. He, *Chin. J. Catal.* **2002**, *06*, 503-506.

[6] a) S. Lee, M. D. Vece, B. Lee, S. Seifert, R. E. Winans, S. Vajda, *ChemCatChem* **2012**, *4*, 1632-1637; b) E. C. Tyo, C. Yin, M. Di Vece, Q. Qian, G. Kwon, S. Lee, B. Lee, J. E. DeBartolo, S. Seifert, R. E. Winans, R. Si, B. Ricks, S. Goergen, M. Rutter, B. Zugic, M. Flytzani-Stephanopoulos, Z. W. Wang, R. E. Palmer, M. Neurock, S. Vajda, *ACS Catal.* **2012**, *2*, 2409-2423; c) I. A. Samek, N. S. Bobbitt, R. Q. Snurr, P. C. Stair, *J. Catal.* **2020**, *384*, 147-158; d) N. F. Dummer, S. Bawaked, J. Hayward, R. Jenkins, G. J. Hutchings, *Catal. Today* **2010**, *154*, 2-6; e) Z. Feng, J. Lu, H. Feng, P. C. Stair, J. W. Elam, M. J. Bedzyk, *J. Phys. Chem. Lett.* **2013**, *4*, 285-291; f) M. Lezanska, G. S. Szymanski, P. Pietrzyk, Z. Sojka, J. A. Lercher, *J. Phys. Chem. C* **2007**, *111*, 1830-1839.

[7] M. Jin, Z. Cheng, X. Jiang, Y. Gao, X. Fang, *Chin. J. Catal.* **2010**, *31*, 1177-1184.

[8] a) A. Halder, M. A. Ha, H. Zhai, B. Yang, M. J. Pellin, S. Seifert, A. N. Alexandrova, S. Vajda, *ChemCatChem* **2020**, *12*, 1307-1315; b) L. Li, Q. Yang, S. Chen, X. Hou, B. Liu, J. Lu, H. L. Jiang, *Chem. Commun.* **2017**, *53*, 10026-10029.

[9] a) H. Feng, J. W. Elam, J. A. Libera, M. J. Pellin, P. C. Stair, *J. Catal.* **2010**, *269*, 421-431; b) S. Lee, A. Halder, G. A. Ferguson, S. Seifert, R. E. Winans, D. Teschner, R. Schlogl, V. Papaefthimiou, J. Greeley, L. A. Curtiss, S. Vajda, *Nat. Commun.* **2019**, *10*, 954-963; c) B. Sarkar, C. Pendem, L. N. S. Konathala, T. Sasaki, R. Bal, *Catal. Commun.* **2014**, *56*, 5-10; d) X. Chen, X. Su, H. Duan, B. Liang, Y. Huang, T. Zhang, *Catal. Today* **2017**, *281*, 312-318.

[10] a) A. Ebadi, N. Safari, M. H. Peyrovi, *Appl. Catal. A* **2007**, *321*, 135-139; b) S. Goergen, C. Yin, M. Yang, B. Lee, S. Lee, C. Wang, P. Wu, M. B. Boucher, G. Kwon, S. Seifert, R. E. Winans, S. Vajda, M. F. Stephanopoulos, *ACS Catal.* **2013**, *3*, 529-539.

[11] a) W. Qi, D. S. Su, *ACS Catal.* **2014**, *4*, 3212-3218; b) Y. Cao, H. Yu, H. Wang, F. Peng, *Catal. Commun.* **2017**, *88*, 99-103; c) L. He, W. C. Li, S. Xu, A. H. Lu, *Chemistry* **2019**, *25*, 3209-3218; d) Y. Lin, Z. Liu, Y. Niu, B. Zhang, Q. Lu, S. Wu, G. Centi, S. Perathoner, S. Heumann, L. Yu, D. S. Su, *ACS Nano* **2019**, *13*, 13995-14004; e) J. Zhu, A. Holmen, D. Chen, *ChemCatChem* **2013**, *5*, 378-401; f) S. Navalon, A. Dhakshinamoorthy, M. Alvaro, M. Antonietti, H. Garcia, *Chem. Soc. Rev.* **2017**, *46*, 4501-4529.

[12] W. Qi, P. Yan, D. S. Su, *Acc. Chem. Res.* **2018**, *51*, 640-648.

[13] a) S. Navalón, A. Dhakshinamoorthy, M. Álvaro, H. García, *Chem. Mater.* **2020**, *32*, 4116-4143; b) X. Duan, W. Tian, H. Zhang, H. Sun, Z. Ao, Z. Shao, S. Wang, *ACS Catal.* **2019**, *9*, 7494-7519.

[14] D. S. Su, N. I. Maksimova, G. Mestl, V. L. Kuznetsov, V. Keller, R. Schlögl, N. Keller, *Carbon* **2007**, *45*, 2145-2151.

[15] X. Liu, B. Frank, W. Zhang, T. P. Cotter, R. Schlögl, D. S. Su, *Angew. Chem. Int. Ed.* **2011**, *50*, 3318-3322.

[16] X. Sun, Y. Ding, B. Zhang, R. Huang, D. S. Su, *Chem. Commun.* **2015**, *51*, 9145-9148.

[17] X. Sun, R. Wang, B. Zhang, R. Huang, X. Huang, D. S. Su, T. Chen, C. Miao, W. Yang, *ChemCatChem* **2014**, *6*, 2270-2275.

[18] a) D. S. Su, S. Perathoner, G. Centi, *Chem. Rev.* **2013**, *113*, 5782-5816; b) Y. Lin, X. Sun, D. S. Su, G. Centi, S. Perathoner, *Chem. Soc. Rev.* **2018**, *47*, 8438-8473; c) R. Wang, X. Sun, B. Zhang, X. Sun, D. S. Su, *Chem. Eur. J.* **2014**, *20*, 6324-6331.

[19] W. Shan, S. Li, X. Cai, J. Zhu, Y. Zhou, J. Wang, *ChemCatChem* **2018**, *11*, 1076-1085.

[20] a) F. Huang, Y. Deng, Y. Chen, X. Cai, M. Peng, Z. Jia, P. Ren, D. Xiao, X. Wen, N. Wang, H. Liu, D. Ma, *J. Am. Chem. Soc.* **2018**, *140*, 13142-13146; b) F. Huang, Y. Deng, Y. Chen, X. Cai, M. Peng, Z. Jia, J. Xie, D. Xiao, X. Wen, N. Wang, Z. Jiang, H. Liu, D. Ma, *Nat. Commun.* **2019**, *10*, 4431-4436.

[21] S. L. Nauert, A. S. Rosen, H. Kim, R. Q. Snurr, P. C. Stair, J. M. Notestein, *ACS Catal.* **2018**, *8*, 9775-9789.

[22] M. Jin, P. Lu, G. X. Yu, *Adv. Mater. Res.* **2012**, *550*, 379-382.

[23] H. Zhu, Q. Ge, W. Li, X. Liu, H. Xu, *Catal. Lett.* **2005**, *105*, 29-33.

[24] H. M. AbdelDayem, *Adsorpt. Sci. Technol.* **2004**, *22*, 755-772.

[25] a) L. I. Ali, A. G. A. Ali, S. M. Aboul-Fotouh, A. K. Aboul-Gheit, *Appl. Catal. A* **1999**, *177*, 99-110; b) P. Tomkins, A. Mansouri, V. L. Sushkevich, L. I. van der Wal, S. E. Bozbag, F. Krumeich, M. Ranocchiari, J. A. vanBokhoven, *Chem. Sci.* **2019**, *10*, 167-171.

[26] J. Zhang, X. Liu, R. Blume, A. Zhang, R. Schlogl, D. S. Su, *Science* **2008**, *322*, 73-77.

[27] C. Portet, G. Yushin, Y. Gogotsi, *Carbon* **2007**, *45*, 2511-2518.

[28] J. H. Zhou, Z. J. Sui, J. Zhu, P. Li, D. Chen, Y. C. Dai, W. K. Yuan, *Carbon* **2007**, *45*, 785-796.

Entry for the Table of Contents

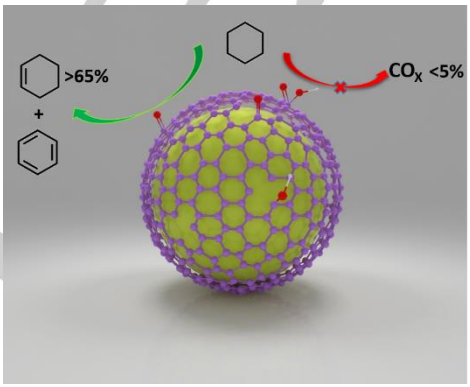

CO_x resistant ODH of cyclohexane was achieved on a metal-free nanodiamonds (NDs) catalysts with a sp^3@sp^2 hybrid structure, as a green production of cyclohexene with low CO_x emission. The selectivity of cyclohexene can reach as high as 67% with significantly suppressed CO_x emission (< 5%), which is on top of the highest reported values among other metal(oxide)/metal-free catalysts. The strained sp^3@sp^2 core-shell structure of NDs favors the surface nucleophilic groups that promotes C-H bond dissociation over C-C bond breaking. Kinetic studies further reveal that deep oxidation of both cyclic hydrocarbons is largely suppressed due to the low density of electrophilic functional groups.